Front. Optoelectron. 2014, 7(3): 265–276
DOI 10.1007/s12200-014-0420-8

REVIEW ARTICLE

# Low phase noise hybrid silicon mode-locked lasers

**Sudharsanan SRINIVASAN (✉)[1], Michael DAVENPORT[1], Martijn J. R. HECK[2], John HUTCHINSON[3], Erik NORBERG[3], Gregory FISH[3], John BOWERS[1]**

1 Department of Electrical and Computer Engineering, University of California, Santa Barbara CA 93106, USA
2 Department of Engineering, Aarhus University, Aarhus, Denmark
3 Aurrion Inc., Goleta CA 93117, USA



**Abstract** In this paper, we review recent results on hybrid silicon mode-locked lasers with a focus on low phase noise optical pulse generation. Taking a high level design approach to lowering phase noise, we show the need for long on-chip optical delay lines for mode-locked lasers to reach and overcome material limits. Key results include demonstration of the longest (cavity length 9 cm) integrated on-chip mode locked laser, 14 dB reduction of Lorentzian noise on a 20 GHz radio-frequency (RF) signal, and greater than 55 dB optical supermode noise suppression using harmonically mode locked long cavity laser, 10 GHz passively mode locked laser with 15 kHz linewidth using on-chip all optical feedback stabilization.

**Keywords** optoelectronic devices, mode-locked lasers, semiconductor lasers

## 1 Introduction

Mode-locked laser diodes (MLLDs) are gaining interest as compact microwave signal sources for high bit rate communication systems, optically sampled analog to digital converters (ADCs), frequency metrology, and arbitrary waveform generation. In the case of ADCs, the aperture jitter present in complementary metal-oxide-semiconductor (CMOS) and SiGe electronic technology, which is around 1 ps [1], is a major limiting factor in reaching higher sampling rate and resolution. Figure 1 shows the requirement for timing jitter of the source versus sampling frequency for different number of resolving bits. This dictates that for an 8 bit resolved ADC, the timing jitter should be 100 fs or less for sampling frequencies in the X/Ku band.

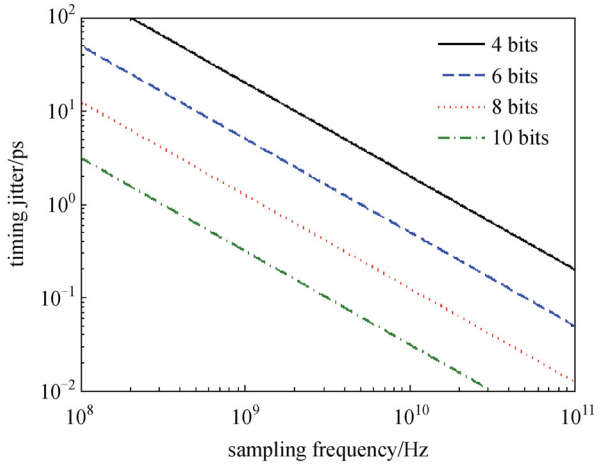


**Fig. 1** Plot of timing jitter requirement versus sampling rate for different bits of resolution

The short cavities of MLLDs enable very high repetition rates, such as ~100 GHz demonstrated in Ref. [2]. They are also robust and have long lifetimes. This is particularly an important feature for low-noise lasers as they require minimum start-up and monitoring. Monolithic semiconductor lasers usually consume much less power than their bulk counterparts with assembled components. Semiconductor manufacturing techniques allow for large scale production of these lasers with tightly controlled performance variations.

Despite all the beneficial factors listed above, there have been only a few demonstrations where high frequency operation and low timing jitter have been simultaneously achieved [3–6]. Moreover, these demonstrations often involve external cavity arrangements that are not readily scalable in terms of large scale manufacturing. To drive down cost, we need to integrate the external cavity elements on-chip. Two suggested substrates for integration

Received February 15, 2014; accepted March 11, 2014

E-mail: sudhas@ece.ucsb.edu

include InP and Si. Although a variety of active and passive elements, viz. laser, amplifier, filter, multiplexer etc., have been integrated on InP substrates, the cost is still limited by the substrate sizes. The hybrid silicon platform [7] based on oxygen plasma assisted wafer bonding [8] allows for fabrication of both active and passive elements on large substrates (200 mm or more), and therefore has attracted many researchers to utilize this technology for various applications from telecommunications to sensing. It also allows for close integration with electronic integrated circuits to lower losses and increase performance [9]. Figure 2(a) shows a photograph of a 200 mm silicon-on-insulator (SOI) wafer before bonding with pre-patterned waveguide circuits with long delay lines and Fig. 2(b) is a schematic of the cross-section of the gain section showing evanescent coupling to the quantum well active region. In this paper, we will review our progress in monolithic integration of mode locked lasers using the hybrid silicon platform and show the utility of long delay lines in reducing microwave phase noise. All the lasers have an eight quantum well active region sandwiched between two 125 nm 1.3Q separate confinement heterostructure (SCH) layers, with a photoluminescence (PL) peak around 1550 nm and allow for a reasonable one-to-one correspondence.

Following the demonstrations of the first hybrid silicon MLLDs in 2007–2008 [10,11], we have progressively investigated the performance of fabricated extended cavity MLLDs to reduce timing jitter while maintaining the repetition rate in the range of 8 to 20 GHz. Our focus is passively mode locked lasers for microwave signal generation. We compare linear to ring cavity designs, short and long cavity designs, and cavities with and without intracavity filters. We also compare passive to active mode locked lasers. After presenting the structures and results, we discuss the comparisons and finally summarize our conclusions.

## 2 Device designs and measurement results

### 2.1 Colliding pulse mode locked laser: linear and ring cavity

A key requirement to integrating lasers with other passive elements on the silicon layer is to efficiently transfer the hybrid mode inside the gain section (see Fig. 2(b)) to the fundamental mode in the silicon waveguide. This is achieved by tapering the III-V mesa structure gradually to a width limited by the resolution and alignment tolerance of the lithography tool. The silicon waveguide width underneath can also be altered to draw the mode center toward or away from the silicon waveguide. This is an essential advantage of this platform and can reduce reflections at the taper tip and also alter the confinement of the optical mode in the quantum wells and thereby change the round trip gain or loss. Some mode locked lasers have gain regions everywhere, but with segmented contacts for active or passive mode locking [10,11]. These designs suffer from excess self phase modulation and excess dispersion. The lasers described here use tapers between gain regions and low loss passive waveguides with lower loss, dispersion, free carrier absorption and two photon absorption, thereby reducing the net spontaneous emission noise.

The first device is a linear cavity colliding pulse mode-locked hybrid silicon laser [12] that incorporates a passive waveguide section as shown in Fig. 3. The laser consists of a 1 mm hybrid silicon/III–V active section with 1.5 mm of silicon waveguide on either side adding up to a total cavity length of 4 mm corresponding to a fundamental repetition rate of 9.16 GHz. The silicon waveguide facets are polished, forming the laser cavity. Centered in the gain section is a 30 μm saturable absorber, allowing for operation in a colliding pulse mode-locking regime, i.e., operating at 18.32 GHz. The optical spectrum from the

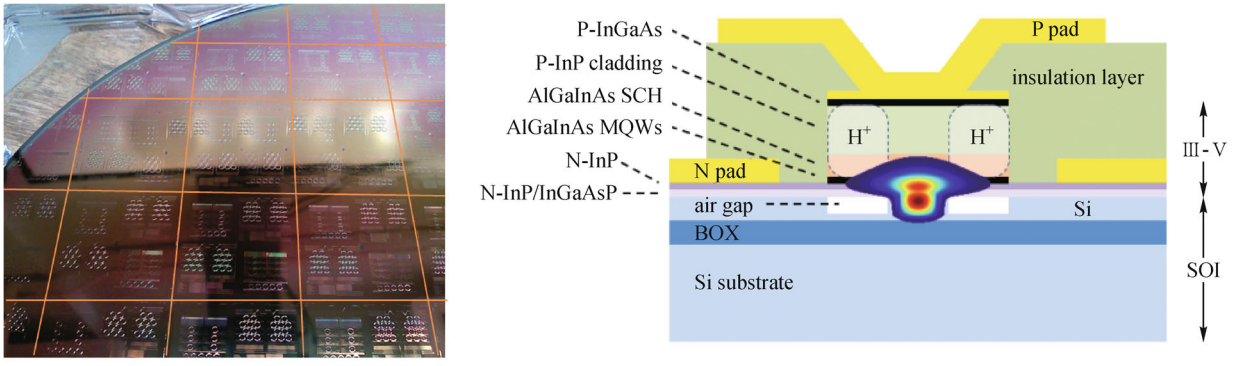


**Fig. 2** (a) Photograph of 200 mm SOI wafer with pre-patterned waveguides. The orange lines have been added to demarcate die boundaries; (b) schematic cross-section of the gain section identifying the different layers with the optical mode overlaid

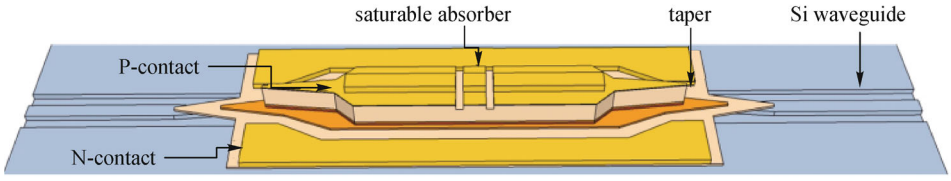


**Fig. 3** Schematic diagram of colliding pulse mode-locked laser with an isolated saturable absorber in the middle

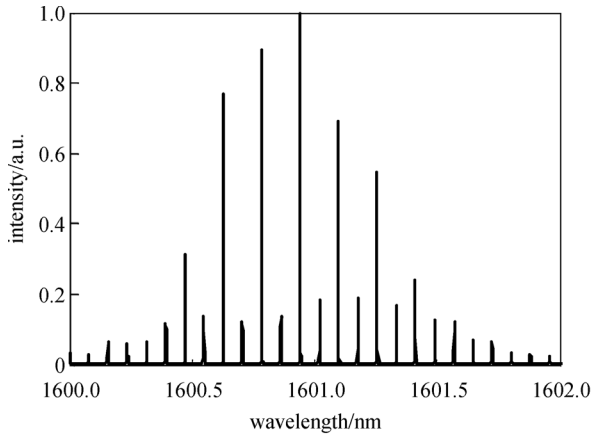


**Fig. 4** Optical spectrum of the laser shown in Fig. 3 with nearly 10 dB of supermode suppression [12]

laser, when the gain section was biased with 96 mA and the saturable absorber was at −3 V, is shown in Fig. 4. No microwave signal is applied to the absorber. The spectrum shows colliding pulse operation with the evidence from enhancement of modes spaced twice the fundamental frequency of the cavity. The optical bandwidth is 100 GHz. On-chip mirrors, described below, would provide control of repetition frequency and increase supermode suppression because the position of the saturable absorber is precisely in the center of the cavity.

The output of the laser diode was detected using a 50 GHz photodiode and observed on an electrical spectrum analyzer (ESA) (see Fig. 5(a)). The power at the fundamental frequency of the cavity, 9.16 GHz, is suppressed to 30 dB below the second harmonic. The 3 dB radio-frequency (RF) linewidth was 250 kHz. Figure 5(c) shows the single sideband phase noise of the microwave signal at 18.32 GHz. The corner frequency as defined by the intersection of the shot noise floor and the $1/f^2$ noise is at 200 MHz.

The second device is a ring cavity mode-locked laser (see Fig. 6), which consists of a 4 mm long ring resonator on silicon coupled to a bus waveguide using an 85/15 multi-mode interference (MMI) coupler. A 1 mm long hybrid silicon/III–V active section of the ring resonator provides gain. The saturable absorber is 50 μm long and centered in the semiconductor optical amplifier (SOA) for stable mode locking operation [13]. The output waveguides are angled and anti-reflection coated to minimize reflections.

The cavity length of this laser is precisely determined compared to the earlier case, which depended on the location of the polished facets. The laser showed lower optical bandwidth, as shown in Fig. 7(a). The gain section was biased with 189 mA and the saturable absorber was at 0 V. The fiber coupled output power was 1 mW with an estimated 6 dB coupling loss. The electrical spectrum in Fig. 7(b) is obtained from collecting the laser output using a 50 GHz photodiode followed by 21 dB RF gain to lift the spurs above noise floor. We see two tones corresponding to the fundamental and its harmonic. Additionally we see spurs at ~1.5 GHz and its beat note (~18.5 GHz) with the

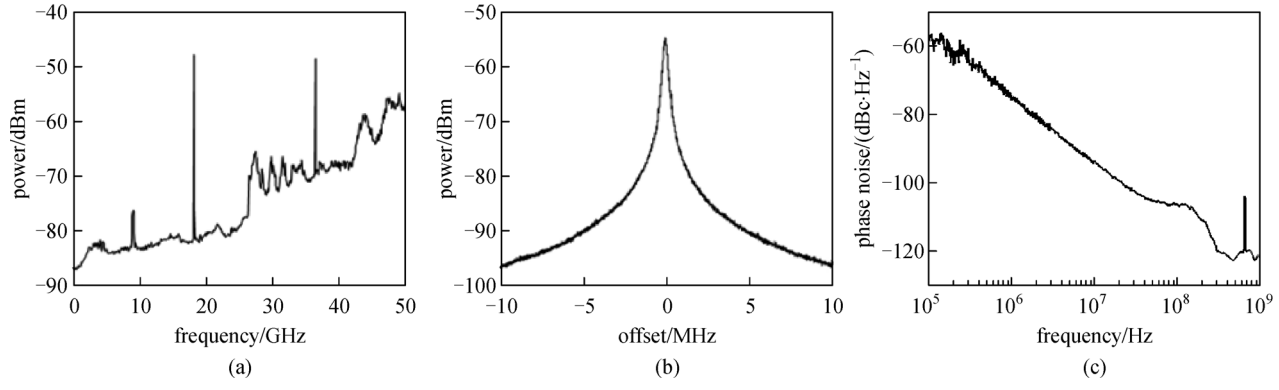


**Fig. 5** (a) Electrical spectrum of the laser shown in Fig. 3 with 30 dB suppression of the fundamental; (b) detailed view of the RF peak at 18.32 GHz. Resolution bandwidths in (a) and (b) are 2 MHz and 20 kHz respectively [12]; (c) single side-band phase noise of 18.32 GHz signal


**Fig. 6** (a) Photograph of the ring cavity colliding pulse mode-locked laser. The letters are added for clarity and denote the P and N contacts for the centered absorber and the two gain sections on either side; (b) schematic of the gain, absorber and waveguide sections inside the laser cavity. SA-saturable absorber, SOA-semiconductor optical amplifier

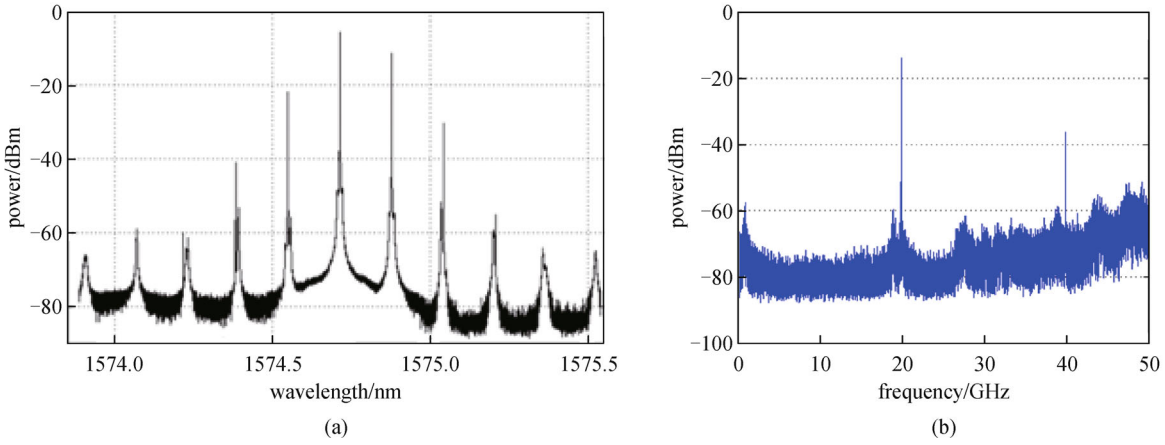


**Fig. 7** (a) Optical spectrum of the ring cavity laser showing 20 GHz spaced optical lines (resolution bandwidth 20 MHz) and (b) electrical spectrum showing the fundamental and its harmonic. Notice the spurs at 1.5 and 18.5 GHz

fundamental, within the analyzer bandwidth. The power at these spurs increases with increasing injection current into the SOA. We believe these spurs are due to a group of optical modes that not locked with the main group of modes and have a pulse repetition rate offset of ~1.5 GHz from the fundamental frequency. The 3 dB RF linewidth was 1.5 MHz, significantly larger than the previous case because of the longer absorber length and the detrimental effect of the parasitic pulse, i.e., through cross-phase and cross-amplitude modulation. The corner frequency for a given phase noise floor, i.e., RF power, however, is similar to the previous device, as this parameter depends on cavity length and total internal round-trip loss.

Both these lasers form an essential building block to realizing complex photonic circuitry using mode-locked lasers. The major pulse broadening effects are spectral gain narrowing, caused by the finite gain bandwidth of the laser medium, and cavity dispersion. We hypothesize the limitation in optical bandwidth is coming from the tapers that not only control propagation loss, across wavelength, through mode mismatch but also through absorption by the quantum wells if insufficiently pumped. The net effect is the lasing wavelength is red-shifted, and the excitation of higher order modes modulates the gain spectrum across wavelength. The optical and the RF linewidth on the other hand can be reduced by increasing the cavity length, which takes us to our next sub-section on long cavity mode-locked lasers.

### 2.2 Long cavity mode locked lasers

We will present results from two long cavity MLLDs with cavity lengths of 9 cm [14] and 4 cm respectively, of which the longer cavity is to our knowledge the longest ever

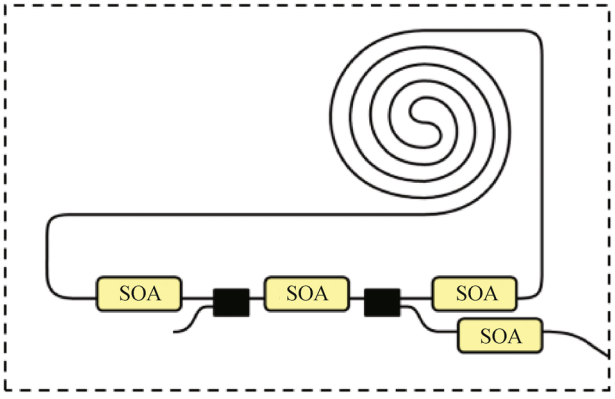


**Fig. 8** Schematic of 9 cm long actively mode-locked laser showing the various active and passive components. Black lines–silicon waveguides, black box–50/50 MMI couplers [14]

reported for an integrated MLLD, surpassing the length reported in Ref. [15] by a factor of two. A schematic of the 9 cm long MLLD is shown in Fig. 8. Two 1200 μm SOAs and one 800 μm (center) are located inside the 9 cm ring cavity to provide the gain of the laser. Two 50/50 MMI couplers are used to couple light out of the cavity. Booster SOAs are located at the output waveguides, which have a 7° angled facet and an anti-reflection coating for minimizing reflections back into the laser cavity. The size of the chip is 0.6 cm × 1 cm.

The SOI passive waveguide loss is around 1.7 dB/cm and the SOA maximum gain is around 6 dB for the 800 μm SOA and 8 dB for the 1200 μm SOA, limited by the heating of the device. The laser is operated at injection currents of 280 and 160 mA for the 1200 and 800 μm SOAs respectively. Under continuous-wave operation, the device lases at 1575 nm. The optical linewidth is less than 7 MHz, as measured by a heterodyne technique.

The laser is actively mode-locked by applying an RF-signal to the 800 μm center SOA inside the laser cavity. The optical spectrum around 1575 nm broadens to about 0.1 nm when 12 dBm of RF-power at 927 MHz is applied. A second group of modes is visible around 1578 nm, 30 dB below the main group of modes, as shown in Fig. 9(a). The output of the laser is amplified by an L-band amplifier and a 50 GHz photodiode is used to record the RF spectrum on an ESA. The spectrum shows a distinct comb of modes for a drive power of 20 dBm, as shown in Fig. 9(b). A supermodulation envelope with a period of around 15 GHz is visible. The harmonics show a side-peak at ~60 MHz higher frequency, which rises at the expense of the main peaks for increasing frequency. We hypothesize that these side-peaks arise as a result of the small group of modes around 1578 nm, which travel at a different group velocity and are likely not synchronized with the main group of modes. The interference between these two groups of modes may explain the 15 GHz supermodulation.

The pulse shape was examined using a digital component analyzer (DCA) with 53 GHz bandwidth. Figure 9(c) shows pulses with duration of about 200 ps and a 1.1 ns period. Given the optical bandwidth of 0.1 nm, the pulses are highly chirped, which is due to the dispersive 9 cm long cavity. In Fig. 10(a), the RF spectrum for locking at the 8th harmonic is shown. The spectrum was optimized for minimization of the supermodes, i.e., the modes in between the harmonics. The power at the supermode frequencies can be suppressed to 30 dB below the power at the locking frequency. The single side-band phase noise of the fundamental and the 8th harmonic are plotted in Fig. 10(b). For frequencies below 30 kHz, the phase noise of the synthesizer dominates. The effect of the long cavity is evident in the corner frequency, which is roughly a factor of 20 better than the lasers in Section 2.1. The quadratic scaling of phase noise with harmonic number is also evident with an 18 dB increase in the phase noise at all offsets.

The second device is a 4 cm long passively mode-locked laser [16]. This laser has a 30 μm long centered absorber in a single 1500 μm long gain section as shown in the schematic of Fig. 11. Light from the ring laser is coupled out to a bus waveguide using directional couplers with a 10:90 splitting ratio. The output waveguides have a 7° angled facet and an anti-reflection coating for minimizing reflections back into the laser cavity. The device size is 7 mm × 1.5 mm.

The output light (CCW) is fed into a 50 GHz photodetector followed by an RF amplifier (18 dB gain, 25 GHz bandwidth) and an ESA. Figure 12 shows data from a high resolution optical spectrum analyzer (RBW-20 MHz), an electrical spectrum analyzer and an autocorrelator, all at 140 mA of SOA current and −1.3 V on the absorber. The time-bandwidth product (TBP) is 1.8, indicating that the pulse is chirped. The electrical spectrum shows equidistant peaks at multiples of 1.99 GHz. The RF linewidth (3 dB) of the 1.99 GHz signal is roughly 14 kHz.

The laser is actively mode-locked at higher harmonics, to generate high repetition rate pulses, by modulating the absorber. The best harmonic mode locking was seen at 7.96 GHz (the 4th harmonic); both in terms of pulse train quality and suppression of the fundamental tone

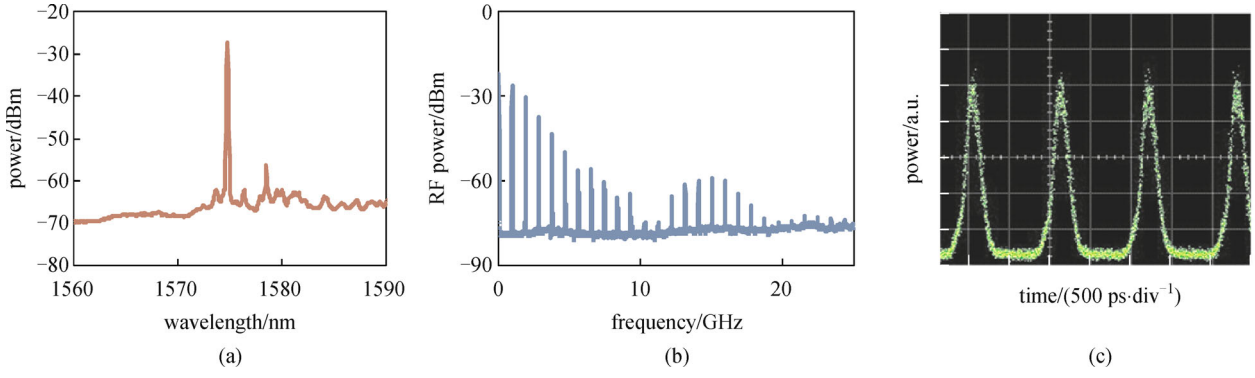


**Fig. 9** (a) Optical spectrum at 12 dBm RF-power at 927 MHz. The resolution bandwidth used was 0.06 nm; (b) RF-spectra obtained at 20 dBm RF-power. Resolution bandwidth was 5 MHz; (c) corresponding time-domain trace obtained with a 53 GHz DCA [14]

(1.99 GHz) on the ESA (see Fig. 13(a)). However, the optical spectrum (see Fig. 13(b)) reveals that the power in the supermode noise spurs is significant compared to the power in the main group of modes, with only a 10 dB reduction seen near the peak of the spectrum. The bias current on the SOA and voltage on the saturable absorber was the same as stated in the passively locked case.

For the 10th harmonic, the RF input power was increased to 10 dBm and a maximum of 25 dB suppression of all other harmonics was achieved. However, the optical spectrum shows near to no suppression of the supermodes noise spurs as seen in Fig. 13(d). The SOA bias current was 206 mA and the saturable absorber voltage is −1.4 V. Unlike a fundamental mode-locked laser, the distribution

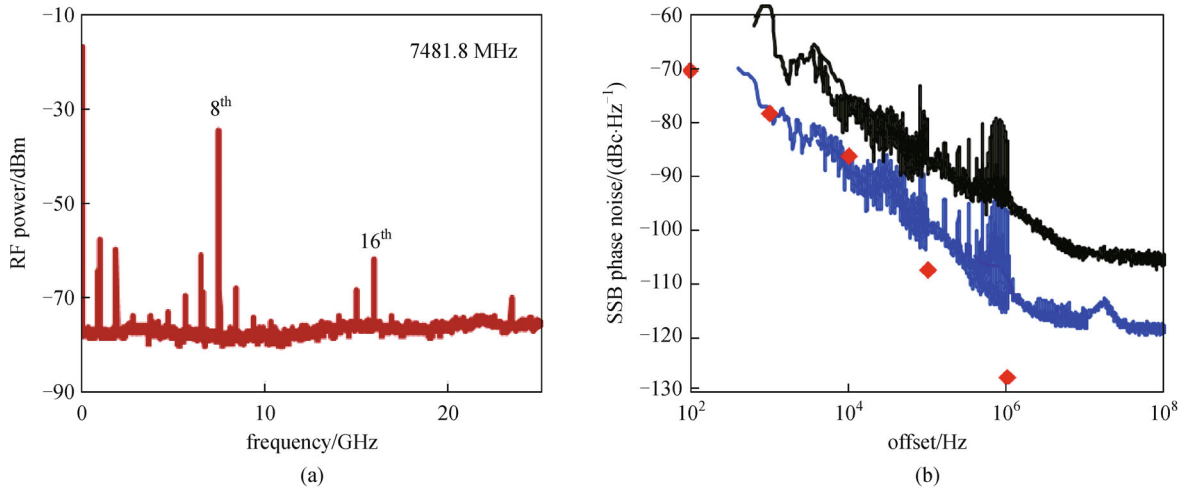


**Fig. 10** (a) RF-spectra obtained with 20 dBm injection at 7481.8 MHz (8th harmonic). Resolution bandwidth was 5 MHz [14]; (b) single sideband phase noise for fundamental (blue) and 8th (black) harmonic mode-locking. Red diamonds show the synthesizer floor specified at 1 GHz

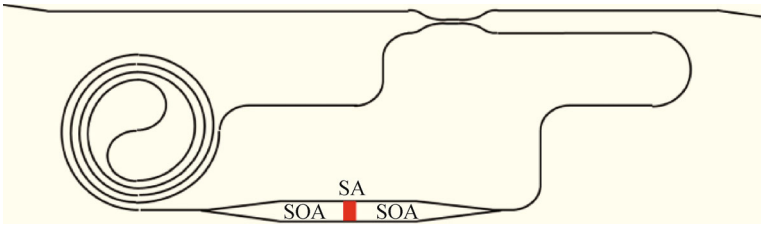


**Fig. 11** Schematic of 4 cm long ring cavity colliding pulse mode-locked laser showing the various active and passive components. Black lines–silicon waveguides, SA-saturable absorber, SOA-semiconductor optical amplifier [16]

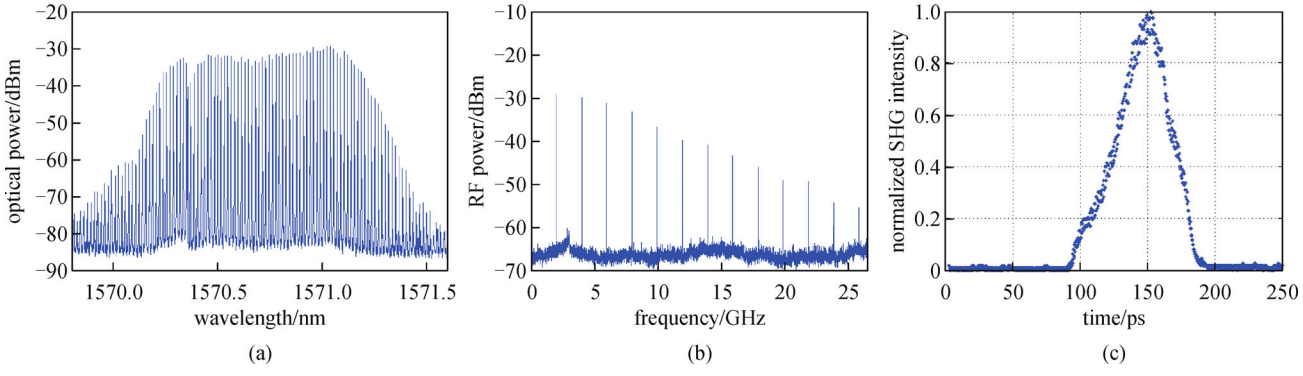


**Fig. 12** (a) Optical spectrum of 2 GHz ring cavity passively mode locked laser showing equally spaced optical lines (resolution bandwidth 20 MHz); (b) electrical spectrum showing the fundamental and its harmonics and (c) autocorrelation trace of the optical output [16]

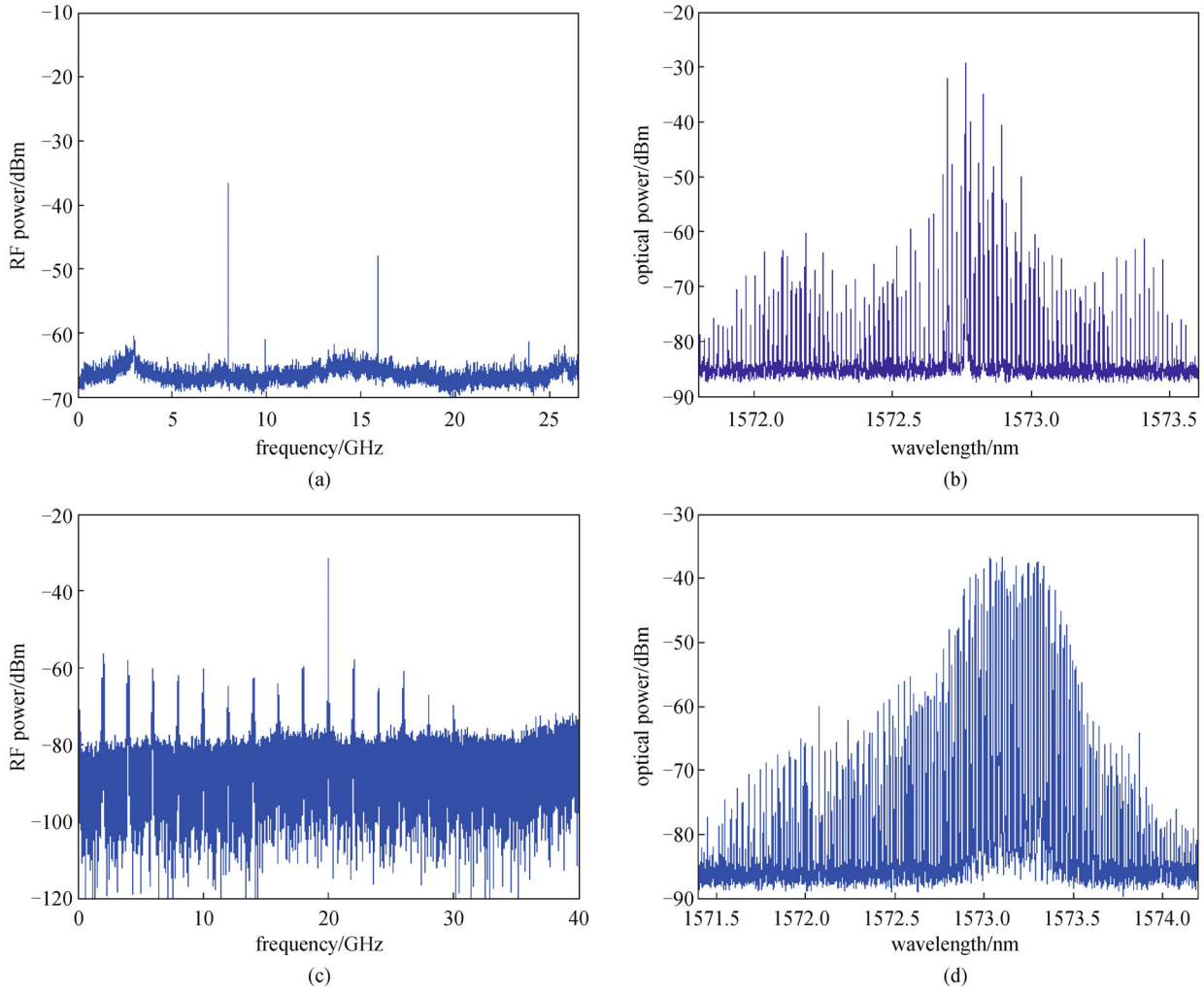


**Fig. 13** Hybrid mode locking results for 2 GHz cavity laser. (a) and (c) show the RF spectra obtained with 0 dBm injection at 7.96 GHz (the 4th harmonic) and 10 dBm injection at 20 GHz (the 10th harmonic) respectively. Resolution bandwidth was 3 MHz; (b) and (d) show the corresponding optical spectra with a resolution bandwidth of 20 MHz [16]

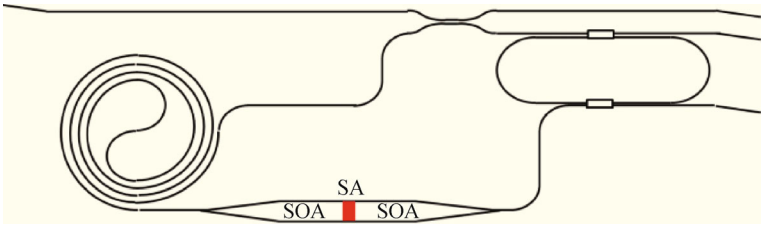


**Fig. 14** Schematic of 4 cm long ring cavity colliding pulse mode-locked laser showing the various active and passive components. Black lines–silicon waveguides, SA-saturable absorber, SOA-semiconductor optical amplifier [16]

of energy among the optical modes in a harmonically mode-locked laser depends on the distribution of spectral phase. To achieve perfect harmonic mode-locking, the spectral phase has to be constant across all the modes. Supermode noise is an undesired feature of all harmonically mode-locked long cavity lasers and contributes to the integrated timing jitter. We now show that this can be resolved with the following laser designs.

### 2.3 Long cavity mode locked laser with intracavity filter

The laser design shown in Fig. 14 is identical to the previous laser, except that it incorporates a ring resonator inside the cavity which has a FSR that is a multiple of the repetition rate of the laser. In our case, we designed a 20 GHz filter with an FSR that is 10 times the fundamental. The optical and electrical spectrum for passive mode

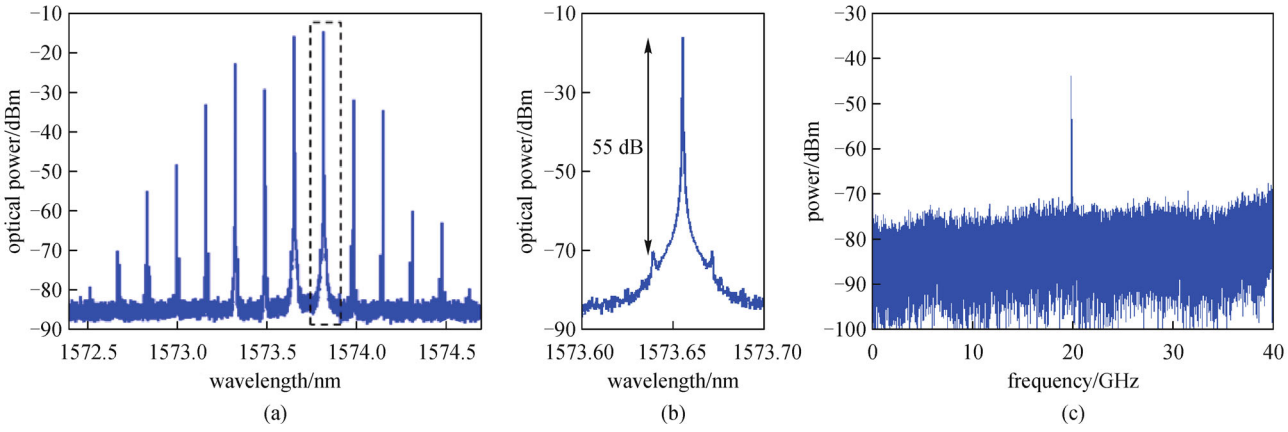


**Fig. 15** (a) Optical spectrum; (b) close-up into the dashed box region in (a) showing 55 dB supermode suppression. Resolution bandwidth was 20 MHz; (c) electrical spectrum for the MLLD with a 20 GHz FSR intra-cavity filter. Resolution bandwidth was 3 MHz [16]

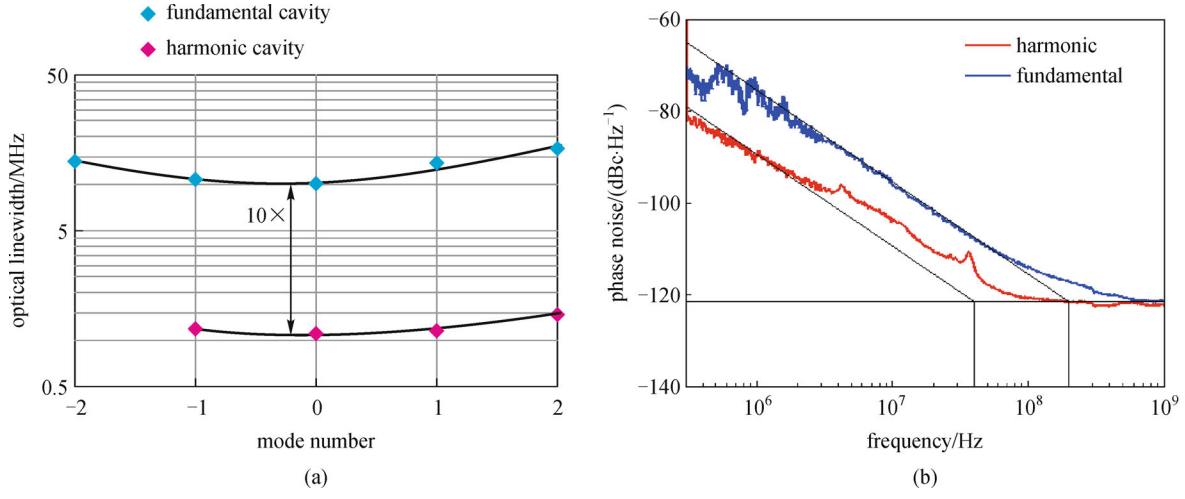


**Fig. 16** (a) Optical linewidth measurement and (b) single sideband phase noise of 20 GHz signal for the fundamental and harmonic MLLDs. The black lines in both plots are a guide to the eye with a slope of 20 dB per decade

locking at an SOA current of 215 mA and absorber voltage of −1.3 V is shown in Fig. 15. With this design, we were able to achieve up to 55 dB optical side mode suppression at the peak of the comb. The ESA shows a clean spectrum with a peak at 19.951 GHz and no harmonics of the 2 GHz cavity seen. The 3 dB RF linewidth estimate is 52 kHz. This result is a factor of 30 better than the linewidth of 1.5 MHz obtained for a passively locked fundamental 20 GHz ring cavity with the same absorber length.

The optical linewidths from a heterodyne measurement are shown in Fig. 16(a), for both this laser and the fundamental 20 GHz ring laser discussed in Section 2.1. We see a 10× improvement in optical linewidth from the increased cavity length. The linewidth also grows quadratically around the central mode as expected. The phase noise of the microwave frequency generated from these two lasers is shown in Fig. 16(b). 20 dB of off-chip optical gain was used in the case of the harmonically mode locked laser for this measurement. The 30× improvement in linewidth shows up as 14 dB (= $10\log_{10}(30)$) improvement in the $1/f^2$ phase noise and a ~5.5× ( = √30) reduction in corner frequency. These results are similar to the state of the art results for semiconductor passively MLLDs.

Furthermore, on driving the absorber with a signal generator, the phase noise close to carrier is reduced as shown in Fig. 17. The total integrated jitter from 10 kHz to 10 GHz is 540 fs. We hypothesize the reason for the peaking at ~7 MHz in Fig. 17 and the deviation from the $1/f^2$ line in Fig. 16(b), is spurious reflections from the tapers within the laser cavity.

### 2.4 Feedback stabilized coupled cavity mode-locked laser

An alternative approach to stabilizing a MLLD is to add a long external cavity, as shown in Fig. 18. The photonic circuit consists of a 10 GHz mode-locked laser and a

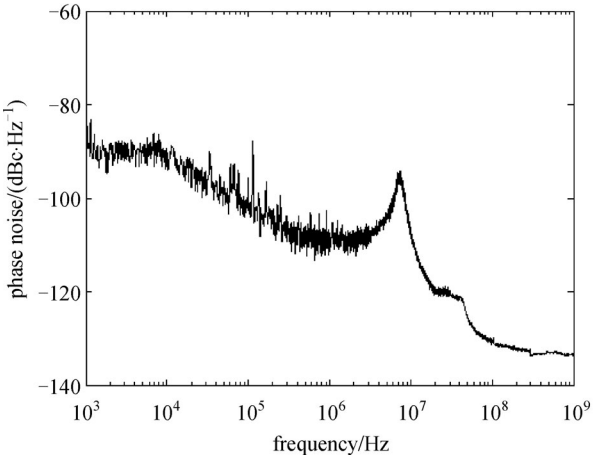


**Fig. 17** Single sideband phase noise of 20 GHz signal for the harmonic MLLD when the saturable absorber is driven with 10 dBm input power

3.855 cm long delay line with a *y*-branch loop mirror at the far end of the spiral. Silicon rib waveguides were used for the passive sections. The MLL is formed by two Sagnac loop mirrors, a 1 mm hybrid silicon/III–V gain section, and a 30 μm saturable absorber in the center of the gain section. The directional coupler based loop mirror allows partial reflection, and is designed for a 50% power reflection coefficient. The taper has 0.9 dB of loss, and a power reflection of 1%.

The coupled cavity is 3.855 cm long and is terminated with a *y*-branch loop mirror that is designed for 100% reflection. This gives the coupled cavity a total round-trip length that is 20 times the length of the mode-locked laser, and a free spectral range of 500 MHz. The loss in the silicon waveguides is 2 dB/cm. To provide an optimal level of feedback, an 800 μm long SOA was placed at the output of the laser to adjust the amplitude and a Ni/Cr heater was used to thermally control the phase in the delay line. The waveguide output is anti-reflection coated with a power reflection coefficient of 0.5%. The coupling loss to the lensed fiber used during measurement is 8 dB.

The passive mode-locked performance of the laser without the coupled cavity was measured by leaving the SOA in the coupled cavity un-biased, which introduces an additional 18 dB loss each way. The feedback in this case is negligible, as verified by adjusting the thermal phase tuner in the coupled cavity does not change the mode-locking behavior. The 3 dB width of the RF peak is 1.06 MHz, shown in red with the label "decoupled" in Fig. 19(a). Next, the SOA and thermal tuner in the coupled cavity were tuned to minimize the RF linewidth down to 15 kHz, shown in blue with the label "coupled." Due to its proximity to the mode-locked laser, activating the SOA causes the operating frequency of the MLL to shift to 9.95 GHz because of thermal crosstalk. The optical spectrum of the laser under optimal bias conditions is shown in Fig. 19(b). The optical linewidth without and with feedback stabilization (see Fig. 19(c)) reduced from ~1 GHz to below the resolution limit of the analyzer (20 MHz).

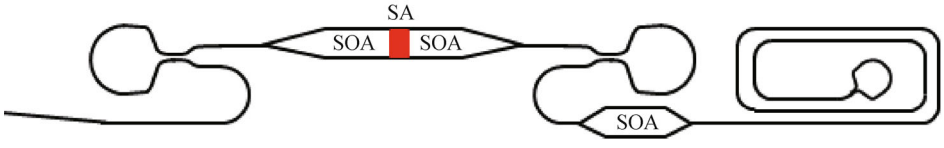


**Fig. 18** Schematic of coupled linear cavity colliding pulse mode-locked laser showing the various active and passive components. Black lines–silicon waveguides, SA-saturable absorber, SOA-semiconductor optical amplifier

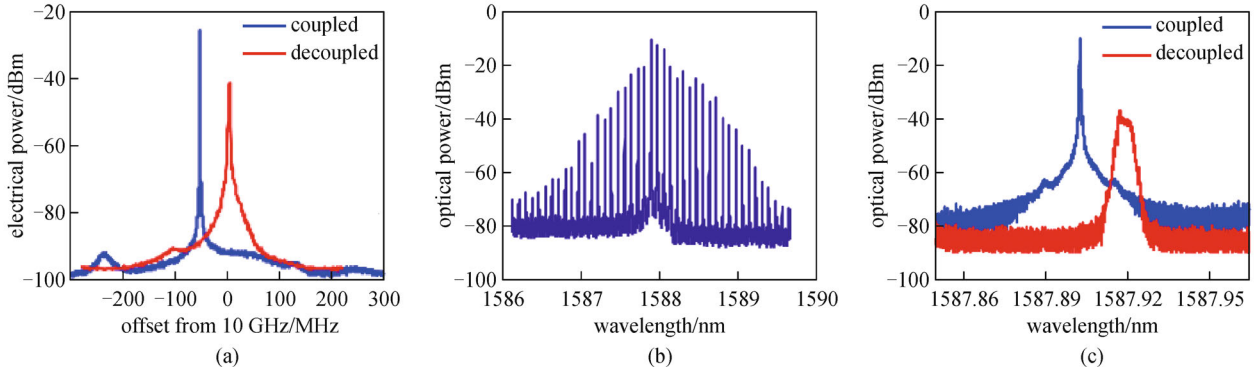


**Fig. 19** (a) RF spectra showing the laser operation with the coupled cavity SOA off ("decoupled") and the SOA biased at 300 mA ("coupled"); (b) wide span view of the optical spectrum in coupled cavity operation and (c) close–up into a single spectral line with and without feedback stabilization

**Table 1** Phase noise data for the various mode locked lasers discussed in the text showing the improvement from long cavity lengths

| No. | laser cavity | | repetition rate/GHz | locking mechanism | phase noise at 1 MHz /(dBc·Hz$^{-1}$) | integrated jitter (100 kHz – 100 MHz)/ps |
|---|---|---|---|---|---|---|
| | type | length/mm | | | | |
| 1 | linear | 4 | 18.32 | passive | −75 | 6.8 |
| 2 | ring | 4 | 19.95 | passive | −75 | 4.31 |
| 3 | ring | 40 | 20 | passive | −90 | 1.3 |
| 4 | ring | 40 | 20 | active | −110 | 0.31 |
| 5 | ring | 90 | 0.927 | active | −110 | 4.04 |
| 6 | ring | 90 | 7.482 | active | −92 | 2.27 |

## 3 Discussion

In this section, we discuss advantages of the various designs, identify bottlenecks and suggest solutions to resolve them. Table 1 shows the phase noise and jitter data for the short cavity and harmonically locked long cavity lasers. The longest cavity (9 cm) showed the lowest corner frequency compared to all other designs. However, to utilize the benefit of the long optical delay for higher frequency generation ($>8$ GHz), we require a mode locked laser design with the intracavity filter to dictate the desired repetition rate while keeping the supermode noise low and stabilize the laser. We demonstrate this in Section 2.3. The root-mean-square (RMS) jitter obtained from integrating the single-sideband phase noise from 100 kHz to 100 MHz, for the intracavity filter based long cavity laser, is 1.3 ps as stated in row 3 of Table 1. The state-of-art passively mode-locked laser shows similar value of jitter (~1.31 ps) in the same frequency range. The fundamental MLLDs shown in Section 2.1 have phase noise levels 30 times worse than the best demonstrated. However, we show that we can overcome this by optimizing the design of the laser at a circuit level.

Although these long cavity lasers are promising, the output power suffers from the excess loss associated with the delay line and the filter. These are useful for complete on-chip processing, which does not suffer from coupling losses. A more desirable design is the coupled cavity MLLD discussed in Section 2.4. This laser has three significant advantages. First, the long delay line and associated losses are external to the main cavity and the output power is significantly higher. Second, the fundamental laser cavity acts as a high quality factor filter to reduce supermode noise. Calculations show that with sufficient feedback strength and proper phase tuning, we should be able to achieve the same improvement in microwave phase noise as in the case with the delay line inside the laser cavity [17]. However, this is yet to be demonstrated. Third, the reflection from the coupled cavity suppresses the influence of taper reflections inside the laser, thereby improving laser stability. The effect of amplifier noise in the coupled cavity to the generated microwave phase noise will be studied in future. This work will also be extended to longer delay line lengths of 1 m or more using low loss nitride waveguides [18] heterogeneously integrated with hybrid silicon gain sections [19] that should reduce the net jitter to below 100 fs.

The presented mode locked laser performance needs improvement in terms of increasing the optical mode comb bandwidth and expanding the region of mode locking in the SOA current vs. saturable absorber voltage bias space. The lasing wavelength is also significantly red shifted from the photoluminescence peak. Inverse Fourier transform applied to optical and electrical spectral data assuming constant phase across all modes suggest the existence of secondary satellite peaks in the pulse train generated in regions around the stable mode locking region. The tapered mode converters are the prime question of study in this regard. We observe that while longer taper lengths are required for low reflections the red shift in lasing wavelength is also proportionally larger. A blunt taper tip also excites unwanted higher order modes. A detailed study on effect of taper length on lasing wavelength and intracavity reflection is underway. Modern deep ultraviolet (DUV) lithography tools should also allow for better alignment and sharper taper tips for efficient mode conversion while keeping the taper lengths short.

## 4 Conclusions

In conclusion, we have reviewed our recent progress in generating low phase noise microwave signals using long cavity mode-locked lasers. Results from the longest on-chip laser cavity mode locked laser showed significant improvement in the corner frequency. We successfully showed that supermode noise from harmonically locking a long laser cavity can be suppressed using an intracavity filter. A novel on-chip feedback stabilized coupled cavity mode locked laser is presented as a promising design solution to preserve high output power while drawing the benefit of long feedback delay to reduce phase noise.

**Acknowledgements** The authors thank Josh Conway and Jag Shah of DARPA, Alex Fang and Eric Hall of Aurrion, Doug Baney and Steve Newton of Agilent, and Daryl Spencer and Jon Peters of UCSB for helpful discussions. The research was supported by DARPA MTO under an EPHI grant.

## References


1. Juodawlkis P W, Twichell J C, Betts G E, Hargreaves J J, Younger R D, Wasserman J L, O'Donnell F J, Ray K G, Williamson R C. Optically sampled analog-to-digital converters. IEEE Transactions on Microwave Theory and Techniques, 2001, 49(10): 1840–1853
2. Rosales R, Merghem K, Martinez A, Accard A, Lelarge F, Ramdane A. High repetition rate two-section InAs/InP quantum-dash passively mode locked lasers. In: Proceedings of 23rd International Conference on Indium Phosphide and Related Materials. Berlin, 2011
3. Jiang L A, Abedin K S, Grein M E, Ippen E P. Timing jitter reduction in modelocked semiconductor lasers with photon seeding. Applied Physics Letters, 2002, 80(10): 1707–1709
4. Drzewietzki L, Breuer S, Elsäßer W. Timing jitter reduction of passively mode-locked semiconductor lasers by self- and external-injection: numerical description and experiments. Optics Express, 2013, 21(13): 16142–16161
5. Lin C Y, Grillot F, Li Y, Raghunathan R, Lester L F. Microwave characterization and stabilization of timing jitter in a quantum-dot passively mode-locked laser via external optical feedback. IEEE Journal on Selected Topics in Quantum Electronics, 2011, 17(5): 1311–1317
6. Fiol G, Kleinert M, Arsenijevic D, Bimberg D. 1.3 μm range 40 GHz quantum-dot mode-locked laser under external continuous wave light injection or optical feedback. Semiconductor Science and Technology, 2011, 26(1): 014006-1 – 014006-5
7. Heck M J R, Bauters J F, Davenport M L, Doylend J K, Jain S, Kurczveil G, Srinivasan S, Tang Y, Bowers J E. Hybrid silicon photonic integrated circuit technology. IEEE Journal of Selected Topics in Quantum Electronics, 2013, 19(4): 6100117-1–6100117-17
8. Liang D, Bowers J E. Highly efficient vertical outgassing channels for low-temperature InP-to-silicon direct wafer bonding on the silicon-on-insulator substrate. Journal of Vacuum Science & Technology B Microelectronics and Nanometer Structures, 2008, 26(4): 1560–1568
9. Sodhi A, Beach S J, Chen L, Jacob-Mitos M, Roth J E, Bowers J, Theogarajan L. Heterogeneous optoelectronic integration using locally polymerized imprinted hard mask. Proceedings of SPIE Optoelectronic Integrated Circuits XV, 2013, 8628: 86280K-1–86280K-8
10. Koch B R, Fang A W, Cohen O, Bowers J E. Mode-locked silicon evanescent lasers. Optics Express, 2007, 15(18): 11225–11233
11. Fang A W, Koch B R, Gan K G, Park H, Jones R, Cohen O, Paniccia M J, Blumenthal D J, Bowers J E. A racetrack mode-locked silicon evanescent laser. Optics Express, 2008, 16(2): 1393–1398
12. Davenport M L, Kurczveil G, Heck M J R, Bowers J E. A hybrid silicon colliding pulse mode-locked laser with integrated passive waveguide section. In: Proceedings of 2012 IEEE Photonics Conference (IPC). Burlingame, CA, 2012, 816–817
13. Bente E A J M, Barbarin Y, Heck M J R, Smit M K. Modeling of integrated extended cavity InP/InGaAsP semiconductor mode-locked ring lasers. Optical and Quantum Electronics, 2008, 40(2–4): 131–148
14. Heck M J R, Davenport M L, Park H, Blumenthal D J, Bowers J E. Ultra-long cavity hybrid silicon mode-locked laser diode operating at 930 MHz. In: Proceedings of Optical Fiber Communication Conference. San Diego, California, 2010, OMI5
15. Cheung S, Baek J H, Soares F M, Scott R P, Zhou X P, Fontaine N K, Shearn M, Scherer A, Baney D M, Yoo S J B. Super-long cavity, monolithically integrated 1-GHz hybrid mode-locked InP laser for all-optical sampling. In: Proceedings of Photonics in Switching. Monterey, California, 2010, PWD2
16. Srinivasan S, Arrighi A, Heck M J R, Hutchinson J, Norberg E, Fish G, Bowers J E. Harmonically mode-locked hybrid silicon laser with intra-cavity filter to suppress supermode noise. IEEE Journal on Selected Topics in Quantum Electronics, 2014, 20(4): 1–8
17. Otto C, Lüdge K, Vladimirov A G, Wolfrum M, Schöll E. Delay-induced dynamics and jitter reduction of passively mode-locked semiconductor lasers subject to optical feedback. New Journal of Physics, 2012, 14(11): 113033
18. Bauters J F, Heck M J R, John D D, Barton J S, Bruinink C M, Leinse A, Heideman R G, Blumenthal D J, Bowers J E. Planar waveguides with less than 0.1 dB/m propagation loss fabricated with wafer bonding. Optics Express, 2011, 19(24): 24090–24101
19. Piels M, Bauters J F, Davenport M L, Heck M J R, Bowers J E. Low-loss silicon nitride AWG demultiplexer heterogeneously integrated with hybrid III–V/silicon photodetectors. Journal of Lightwave Technology, 2014, 32(4): 817–823


**Sudharsanan Srinivasan** received his Bachelors degree with specialization in Engineering Physics from Indian Institute of Technology, Madras, India (July 2009). He is currently pursuing a Ph.D. at the University of California, Santa Barbara. His research interests are in silicon photonics.

**Michael Davenport** received an undergraduate degree in Optical Engineering from the University of Alabama, Huntsville, in 2007, and a Masters degree in Electrical Engineering from the University of California, Santa Barbara, in 2009, where he is currently pursuing the Ph.D. degree in Electrical Engineering. His current research interests include low-noise mode-locked lasers for applications in optical networks microwave photonics, photonic integrated circuits.

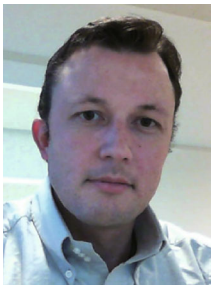

**Martijn J. R. Heck** is an Associate Professor in the Department of Engineering of Aarhus University, where he is starting up a fabless group on photonic integration technologies and applications. He received the M.Sc. degree in Applied Physics and the Ph.D. degree in Electrical Engineering from the Eindhoven University of Technology, the Netherlands, in 2002 and 2008, respec-

tively. From 2007 to 2008, he was a Postdoctoral Researcher at the COBRA Research Institute in Eindhoven, where he was engaged in the development of a technology platform for active–passive integration of photonic integrated circuits. From 2008 to 2009, he was with the Laser Centre, Vrije Universiteit in Amsterdam, the Netherlands, where he was involved in the development of integrated frequency-combs generators. From 2009 to 2013, he was Postdoctoral Researcher and Associate Director of the Silicon Photonics Center at the University of California, Santa Barbara, USA, where he was involved in photonic integrated circuits based on the heterogeneous integration of silicon, silica and III/V photonics. His research interests are photonic integrated circuits fabricated in III/V, silicon and silica platforms and their application to interconnects, microwave photonics, sensors and biomedical imaging and spectroscopy.

**John Hutchinson** is a Staff Process Engineer at Aurrion. Dr. Hutchinson received his Ph.D. from University of California, Berkeley, in Electrical Engineering in 1994. From 1994 to 2008, Dr. Hutchinson was a Staff Engineer at Intel's Components Research department and Optical Platform Division. Prior to Aurrion, Dr. Hutchinson was a Principal Engineer at Emcore working on integrated photonics for telecommunications.

**Erik Norberg** received his Ph.D. in Electrical Engineering from University of California, Santa Barbara (UCSB), in 2011. At UCSB, he developed integrated photonic microwave filters and a high dynamic range integration platform on InP. He is an author/co-author on over 30 papers. Dr. Norberg is currently an Optoelectronic Design Engineer at Aurrion Inc. in Goleta CA, where he is developing integrated Si-photonic systems.

**Gregory Fish** is the Chief Technical Officer at Aurrion. Dr. Fish is considered a leading expert in the field of photonic integration with nearly 20 years of experience in the field of InP based photonic integrated circuits (PICs). He began his work in this area while obtaining a B.S. in Electrical Engineering from the University of Wisconsin at Madison in 1994 and later a M.S. and Ph.D. in Electrical Engineering from the University of California at Santa Barbara in 1999. He is an author/coauthor on over 50 papers in the field and has 12 patents.

**John Bowers** holds the Fred Kavli Chair in Nanotechnology, and is the Director of the Institute for Energy Efficiency and a Professor in the Departments of Electrical and Computer Engineering and Materials at University of California, Santa Barbara (UCSB). He is a cofounder of Aurrion, Aerius Photonics and Calient Networks. Dr. Bowers received his M.S. and Ph.D. degrees from Stanford University and worked for AT& Bell Laboratories and Honeywell before joining UCSB. Dr. Bowers is a member of the National Academy of Engineering and a fellow of the IEEE, OSA and the American Physical Society. He is a recipient of the OSA/IEEE Tyndall Award, the OSA Holonyak Prize, the IEEE LEOS William Streifer Award and the South Coast Business and Technology Entrepreneur of the Year Award. He and coworkers received the EE Times Annual Creativity in Electronics (ACE) Award for Most Promising Technology for the hybrid silicon laser in 2007.

Bowers' research is primarily in optoelectronics and photonic integrated circuits. He has published 10 book chapters, 600 journal papers, 900 conference papers and has received 54 patents. He has published 180 invited papers and conference papers, and given 16 plenary talks at conferences.